Parabolic Renormalization-Group Flow for Interfaces and Membranes

Reinhard Lipowsky[(a)]
Institut für Festkörperforschung, Kernforschungsanlage Jülich GmbH, Postfach 1913, D-5170 Jülich, West Germany
(Received 31 May 1988; revised manuscript received 13 December 1988)

The effective interaction between interfaces or membranes is renormalized by thermally excited shape fluctuations of these surfaces. For a large class of interactions, this renormalization leads to a complex phase diagram which is governed by an unusual renormalization-group flow. This flow exhibits a line of renormalization-group fixed points and leads to essential singularities and nonuniversal critical exponents; it must, however, be distinguished from the well-known Kosterlitz-Thouless flow since it has a parabolic character.

PACS numbers: 05.70.Jk, 68.10.Cr, 87.22.-q

The macroscopic shape of interfaces and membranes reflects their elastic properties. The shape of *interfaces* separating two different phases is controlled by surface (or interfacial) *tension:* For liquids, the tension is isotropic and leads to spherical droplets; for crystals, the tension is anisotropic and can lead to the formation of facets. On the other hand, the shape of *membranes,* which are sheets of amphiphilic molecules, is controlled by *bending rigidity.* This can lead to nonconvex shapes as observed for lipid vesicles and red blood cells.[1]

On mesocopic scales, interfaces and membranes undulate and, thus, change their shape as a result of thermally excited fluctuations.[1-3] In this paper, I will be concerned with fluctuations away from nearly planar surfaces. Then, the elastic energy per unit area is given by $\frac{1}{2}K(\nabla^n l)^2$, where $l(\mathbf{x})$ describes the deviation of the surface shape from its planar reference state. For interfaces, this energy arises from the change in surface area: K is the interfacial stiffness and $n=1$. For membranes, this energy represents the bending energy which is given by the squared mean curvature: K is the bending rigidity and $n=2$.[1,4,5]

In many physical systems, one encounters two or more surfaces which are, on average, parallel. Such a behavior is found, e.g., for (i) wetting, surface melting, and related phenomena; (ii) adhesion of vesicles or biological cells; and (iii) lyotropic liquid crystals consisting of stacks of membranes.[1-3] In all cases, the surfaces experience a mutual *interaction.* The direct interaction $V(l)$ between two *planar* surfaces with separation l reflects the intermolecular forces such as van der Waals electrostatic forces. This interaction has two generic features: (i) It contains a hard wall, i.e., $V(l)=\infty$ for $l<0$ which prevents intersections of the surfaces; and (ii) it decays to zero for large l (in the absence of external forces).

It has been realized recently that the direct interaction $V(l)$ is *renormalized* by the thermally excited shape fluctuations described above. This renormalization can be studied in a systematic way starting from the effective Hamiltonian[6,7]

$$\mathcal{H}\{l\}=\int d^{d-1}x\{\tfrac{1}{2}K(\nabla^n l)^2+V(l)\}, \tag{1}$$

with an implicit small-distance cutoff a, where $l(\mathbf{x})$ now measures the separation of two $(d-1)$-dimensional interfaces or membranes.[5,8] At finite temperature $T>0$, the statistical weight for $l(\mathbf{x})$ is then given by $\exp[-\mathcal{H}\{l\}/T]$

It will be shown below that the models (1) lead to the renormalization-group (RG) flow shown in Fig. 1 whenever $d<2n+1$. The two coordinates, $\rho\sim R$ and $\bar{\rho}\sim\bar{R}$, parametrize the *tails* of $V(l)$ according to[9]

$$V(l)\approx R/l^\tau+\bar{R}l^{\tau-1}\exp[-(l/l_0)^2] \tag{2}$$

for large l, with

$$\tau\equiv 2(d-1)/(2n+1-d). \tag{3}$$

Thus, ρ is the rescaled amplitude of a long-ranged power-law tail while $\bar{\rho}$ is the rescaled amplitude of a short-ranged Gaussian tail. The parabola displayed in Fig. 1 is a line of RG fixed points. This line has two

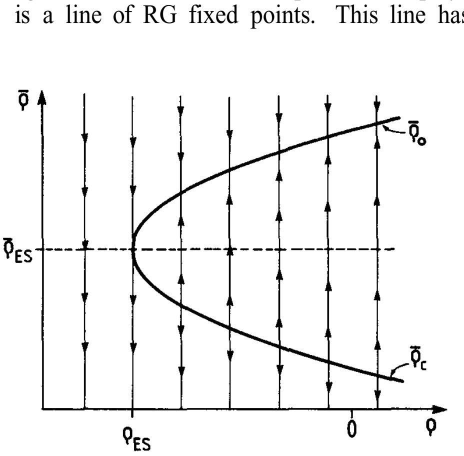

FIG. 1. Parabolic renormalization-group flow in the interaction subspace with coordinates $\rho\sim R$ and $\bar{\rho}\sim\bar{R}$. The line of fixed points has two branches, $\bar{\rho}_0$ and $\bar{\rho}_c$.

branches, $\bar{\rho}=\bar{\rho}_c(\rho)$ and $\bar{\rho}=\bar{\rho}_0(\rho)$, which merge at the bifurcation point $(\rho_{ES},\bar{\rho}_{ES})$ (see Fig. 1). All parameter values which flow into the upper branch $\bar{\rho}_0$ correspond to unbound states of the surfaces. All parameter values which are mapped under the RG to large negative values of $\bar{\rho}$ correspond to *bound states* of the surfaces. The separatrix between these two regions of the $(\rho,\bar{\rho})$ space is the locus of *critical unbinding transitions*. This locus consists (A) of the unique RG trajectory which flows into the bifurcation point $(\rho_{ES},\bar{\rho}_{ES})$, and (B) of the lower branch $\bar{\rho}_c$ of the line of fixed points. The critical behavior along part (A) and part (B) is characterized by essential singularities and by ρ-dependent critical exponents, respectively, see Eqs. (16)-(18) below.

In general, the direct interaction $V(l)$ between two surfaces contains various contributions and, thus, will involve a large number of parameters. However, as far as the *universal* aspects of the critical behavior are concerned, all features of $V(l)$ are *irrelevant* apart from the character of its tail at large l. Now, consider the space of all interactions which behave as $V(l)\approx R/l^\tau + C_W W(l)$ with $R\sim\rho$ for large l. For *each* function $W(l)\ll 1/l^\tau$, the phase diagram in the (ρ,C_W) space is predicted to have the *same topology* as in Fig. 1. This follows from the RG flow which maps all (ρ,C_W) spaces onto the $(\rho,\bar{\rho})$ space shown in Fig. 1: All interactions which correspond to unbound surface states or critical unbinding transitions are again mapped onto the two branches, $\bar{\rho}_0$ and $\bar{\rho}_c$, of RG fixed points. Therefore, the phase diagram in Fig. 1 is not restricted to the interactions given by (2) but applies, in fact, to a *much larger class* of interactions.

The flow shown in Fig. 1 follows from the differential recursion relation

$$\partial\rho/\partial t=0\,,\qquad \partial\bar{\rho}/\partial t=c_1(\rho-\rho_{ES})-c_2(\bar{\rho}-\bar{\rho}_{ES})^2\,, \tag{4}$$

with flow parameter t and $c_1,c_2>0$. This will be derived below from a functional RG approach[6,7,10] which represents an extension of Wilson's approximate recursion relations.[11] In terms of the transformed coordinates, $x\equiv c_2(\bar{\rho}-\bar{\rho}_{ES})$ and $y\equiv x^2-c_1c_2(\rho-\rho_{ES})$, Eq. (4) becomes $\partial x/\partial t=-y$ and $\partial y/\partial t=-2xy$. Then $y=0$ describes the line of fixed points, and the RG trajectories are *parabolas* given by $y=x^2+\text{const}$.[12,13]

It is instructive to compare the flow given by (4) with other RG flows. The critical behavior at a *bulk* critical point is governed by *one* nontrivial RG fixed point.[1,14] On the other hand, the Kosterlitz-Thouless transition also involves a whole line of fixed points. However, if $\tilde{y}=0$ represents this latter line, the associated flow is given by $\partial\tilde{x}/\partial t=-\tilde{y}^2$ and $\partial\tilde{y}/\partial t=-\tilde{x}\tilde{y}$, and the RG trajectories are *hyperbolas* given by $\tilde{y}^2=\tilde{x}^2+\text{const}$ rather than parabolas.

The topologies of the hyperbolic Kosterlitz-Thouless flow and of the parabolic flow derived here are quite different.[12] The separatrix for the hyperbolic flow consists of the fixed-point line with $\tilde{x}<0$ and of *two* straight lines with $\tilde{y}=\pm|c_h|\tilde{x}$. In contrast, the separatrix for the parabolic flow consists of the fixed-point line with $x<0$ and of *one* parabolic piece given by $y=|c_p|x^2$

For infinitesimal rescaling factor $b\to 1+\Delta t$, the functional RG developed in Refs. 6 and 7 leads to

$$\partial V/\partial t=(d-1)V+\zeta l\,\partial V/\partial l + \tfrac{1}{2}v\ln[1+(a_\perp^2/v)\partial^2V/\partial l^2]\,. \tag{5}$$

For the models given by (1), one has $\zeta=0$ for $d\geq 2n+1$ and $\zeta=(2n+1-d)/2>0$ for $d<2n+1$. The parameters $a_\perp^2\sim(T/K)a^{2\zeta}$ and $v\sim T/a^{d-1}$ represent scale factors.[6,10]

A RG fixed point $V^*(l)$ satisfies $\partial V^*/\partial t=0$. It follows from (5) that there is no (nontrivial) fixed point for $\zeta=0$,[6] but a whole line of fixed points for $\zeta>0$.[10] This line has been previously parametrized by the parameter $\sigma>0$ which governs the form of $V^*(l)$ for small l. In terms of the dimensionless variables $z\equiv(2\zeta)^{1/2}l/a_\perp$ and $U(z)\equiv 2\zeta V(l)/v$, the fixed points U^* behave as[10]

$$U^*(z)\approx\sigma/z^\tau+[(\tau+2)/\tau]\ln(z)\ \text{with}\ \sigma>0 \tag{6}$$

for small z, and

$$U^*(z)\approx\rho(\sigma)/z^\tau+\bar{\rho}(\sigma)z^{\tau-1}\exp(-z^2/2) \tag{7}$$

for large z, where the amplitudes ρ and $\bar{\rho}$ are uniquely determined by σ.

Numerical integration of the fixed-point equation reveals (i) that $\rho(\sigma)$ has a unique minimum at $\sigma=\sigma_{ES}$ and, thus, $\rho(\sigma)\approx\rho_{ES}+\frac{1}{2}R_1(\sigma-\sigma_{ES})^2$ close to $\sigma=\sigma_{ES}$; and (ii) that $\rho(\sigma)$ has two zeros at $\sigma=\sigma_{OS}$ and $\sigma=\sigma_{CS}<\sigma_{OS}$. The function $\rho(\sigma)$ is displayed in Fig. 2 and the parameters σ_{ES}, ρ_{ES}, and R_1 are given in Table I for several values of τ. Inspection of this table shows that these parameters are *singular* both at small and at large τ.

The function $\bar{\rho}(\sigma)$ is more difficult to determine ex-

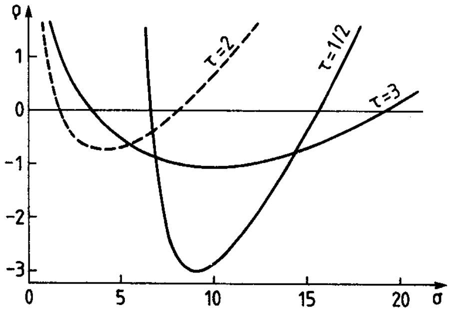

FIG. 2. The function $\rho=\rho(\sigma)$ for $\tau=\frac{1}{2}$, 2, and 3. This function has a unique minimum at $\sigma=\sigma_{ES}$ with $\rho-\rho_{ES}\approx\frac{1}{2}R_1(\sigma-\sigma_{ES})^2$; compare with Table I.

TABLE I. τ dependence (i) of σ_{ES}, ρ_{ES}, and R_1 which characterize the minimum of $\rho(\sigma)$ and (ii) of L and ω/ζ which govern the relevant eigenvalue λ_1, see Eq. (13). The numerical error is of the order of a few percent.

τ	σ_{ES}	$-\rho_{ES}$	R_1	L	ω/ζ
$\frac{1}{8}$	125	21.8	0.17	0.019	0.065
$\frac{1}{4}$	31.5	8.36	0.28	0.059	0.16
$\frac{1}{2}$	9.05	3.00	0.36	0.155	0.37
1	3.83	1.15	0.35	0.313	0.75
2	4.12	0.73	0.14	0.304	1.16
3	9.9	1.06	3.4×10^{-2}	0.134	1.03
4	35	2.37	6.3×10^{-3}	0.040	0.72
8	35700	520	1.5×10^{-6}	4.5×10^{-5}	0.051

cept for $\sigma=\sigma_{OS}$ and $\sigma=\sigma_{CS}$, where $\rho(\sigma)=0$: One finds $\bar{\rho}(\sigma_{OS})>0$ and $\bar{\rho}(\sigma_{CS})<0$ corresponding to a repulsive and an attractive Gaussian tail, respectively. For $\sigma_{CS}<\sigma<\sigma_{OS}$, $\bar{\rho}(\sigma)$ should increase monotonically. Then, the line of fixed points can be rewritten as

$$\rho(\bar{\rho})\approx\rho_{ES}+\tfrac{1}{2}R_2(\bar{\rho}-\bar{\rho}_{ES})^2 \tag{8}$$

for small $\bar{\rho}-\bar{\rho}_{ES}$

The eigenperturbations $f_\lambda(z)$ at the fixed points $U^*(z)$ are governed by

$$[(\tau-\lambda/\zeta)+z\,\partial/\partial z+(1+\partial^2U^*/\partial z^2)^{-1}\partial^2/\partial z^2]f_\lambda(z)=0. \tag{9}$$

Two eigenperturbations can be found exactly: (i) the marginal perturbation $f_0\equiv\partial U^*/\partial\sigma$ with eigenvalue $\lambda=0$ which gives an infinitesimal translation along the line of fixed points; and (ii) the irrelevant (and redundant) perturbation $f_{-\zeta}\equiv\partial U^*/\partial z$ with eigenvalue $\lambda=-\zeta$.

For small z, both f_0 and $f_{-\zeta}$ behave as

$$f_\lambda(z)\sim1/z^{\tau-\lambda/\zeta}. \tag{10}$$

This relation will be imposed, for *all* λ, as the boundary condition for small z. The second, linearly independent solution to (9) blows up exponentially $\sim\exp[(\tau+1)\sigma/z^\tau]$ at small z. Such a perturbation would change the character of the wall region and will be discarded.[15]

For large z, the general solution to (9) behaves as

$$f_\lambda(z)\approx C/z^{\tau-\lambda/\zeta}+Dz^{\tau-1-\lambda/\zeta}\exp(-z^2/2), \tag{11}$$

with $C=C(\sigma,\lambda/\zeta)$. If a relevant perturbation with $\lambda>0$ had a power-law tail $\approx C/z^{\tau-\lambda/\zeta}$, it would dominate the tail of $U^*\approx\rho/z^\tau$. Therefore, the boundary condition at large z is taken to be

$$C(\sigma,\lambda/\zeta)=0 \text{ for } \lambda>0. \tag{12}$$

Numerical integration of (9) shows that there is exactly *one* relevant perturbation, $f_1(z)$, with eigenvalue $\lambda=\lambda_1>0$ for $\sigma<\sigma_{ES}$. As $\sigma\to\sigma_{ES}$ from below, λ_1 goes to zero and f_1 becomes proportional to $f_0=\partial U^*/\partial\sigma$ This implies $C(\sigma_{ES},\lambda_1/\zeta=0)=0$. It then follows from an expansion around the bifurcation point that $\lambda_1/\zeta\approx L(\sigma_{ES}-\sigma)$. On the other hand, one has $\rho-\rho_{ES}\approx\frac{1}{2}R_1(\sigma-\sigma_{ES})^2$ which leads to

$$\lambda_1\approx\omega(\rho-\rho_{ES})^{1/2} \text{ with } \omega/\zeta\equiv L(2/R_1)^{1/2}. \tag{13}$$

The parameters L and ω/ζ as determined from (9) and (12) are given in Table I.

Now, consider $U\equiv U^*+\Delta\bar{\rho}f_1$. Close to the bifurcation point, one then has

$$U(z)\approx\rho(\bar{\rho})/z^\tau+(\bar{\rho}+\Delta\bar{\rho})z^{\tau-1}\exp(-z^2/2) \tag{14}$$

for large z, with $\rho(\bar{\rho})$ as in (8), and terms of $O(\lambda_1\ln(z))$ neglected. Under the RG with rescaling factor b, ρ remains unchanged while $\bar{\rho}+\Delta\bar{\rho}\to\bar{\rho}+b^{\lambda_1}\Delta\bar{\rho}$ for small $\Delta\bar{\rho}$. It then follows from (8) and (13) that ρ and $\bar{\rho}$ are renormalized according to (4) with

$$c_1=\omega/(2R_2)^{1/2} \text{ and } c_2=\tfrac{1}{2}R_2c_1. \tag{15}$$

As the interfaces or membranes unbind, long-ranged correlations build up along the surfaces which are governed by the longitudinal correlation length $\xi_\parallel$. The RG flow given by (4) and (15) implies the following singular behavior for $\xi_\parallel$: (i) Along the branch $\bar{\rho}_c$ with $\rho>\rho_{ES}$, one has $\xi_\parallel\sim(\bar{\rho}-\bar{\rho}_c)^{-\nu_\parallel}$ with

$$\nu_\parallel=1/\lambda_1=1/\omega(\rho-\rho_{ES})^{1/2}. \tag{16}$$

(ii) For $\rho=\rho_{ES}$, integration of (4) gives $t\sim[1/y(t)-1/y(0)]$ with $y\equiv\bar{\rho}-\bar{\rho}_{ES}$. Then, matching at $t=t_m$ with $y(t_m)\sim1$ implies $t_m\sim-1/y(0)$ for small $y(0)$ and

$$\xi_\parallel\sim\exp(t_m)\sim\exp\{2\sqrt{2}/\omega\sqrt{R_2}(\bar{\rho}_{ES}-\bar{\rho})\}, \tag{17}$$

as $\bar{\rho}$ approaches $\bar{\rho}_{ES}$ from below. (iii) For $\rho<\rho_{ES}$, the same matching procedure leads to

$$\xi_\parallel\sim\begin{cases}\exp[2\pi/\omega(\rho_{ES}-\rho)^{1/2}] & \text{for } \bar{\rho}>\bar{\rho}_{ES},\\ \exp[\pi/\omega(\rho_{ES}-\rho)^{1/2}] & \text{for } \bar{\rho}=\bar{\rho}_{ES},\end{cases} \tag{18}$$

as ρ approaches ρ_{ES} from below.

The flow equation (4) has been derived in the vicinity of the bifurcation point at $(\rho_{ES},\bar{\rho}_{ES})$. However, for $\tau=2$, the form of this equation is valid for *all* values of ρ up to a maximal value, $\rho=\rho_{DIS}$. This follows by comparison with the exact critical behavior for wetting transitions with $n=1$ and $d=1+1$.[16] One then finds that the form of the singularities as given by (16)-(18) is *exact* provided $\rho<\rho_{DIS}$. For $\rho>\rho_{DIS}$, one enters subregime (C) of Ref. 16 in which the continuous unbinding transition is preempted by a discontinuous transition.[17,18]

For $\tau=2$, a parabolic RG flow as in (4) gives the exact critical behavior even far away from the bifurcation point. For general τ, $\partial\rho/\partial t=0$ should still apply globally but the flow equation for $\partial\bar{\rho}/\partial t$ should contain correction terms, $(\bar{\rho}-\bar{\rho}_{ES})^m$ with $m=3,4,\ldots$, which will affect the flow far from the bifurcation point. One might hope that such a flow can be calculated perturbatively in the limit of large or small τ. However, for $\tau=\infty$ or $\zeta=0$, only the trivial fixed point $V^*(l)=0$ has been found.[6] Therefore, the evolution of the line of fixed points is highly singular for large τ. Unfortunately, the limit of small τ is also singular as can be seen from Table I. Therefore, a small parameter which allows for a perturbative calculation of the RG flow for interacting surfaces remains to be found.

I thank Daniel M. Kroll for a critical reading of the manuscript.

[a]Present address: Sektion Physik der Universität München, Theresienstrasse 37, D-8000 München, West Germany.

[1]*Physics of Amphiphilic Layers,* edited by J. Meunier, D. Langevin, and N. Boccara, Springer Proceedings in Physics Vol. 21 (Springer-Verlag, Berlin 1987).

[2]"Statistical Mechanics of Membranes and Surfaces," edited by D. R. Nelson (to be published).

[3]*Random Fluctuations and Growth,* edited by G. Stanley and N. Ostrowsky (Kluwer Academic, Dordrecht, 1988).

[4]W. Helfrich, Z. Naturforsch. **28c,** 693 (1973).

[5]In some systems, the stiffness and the rigidity are scale dependent and grow on large scales. Such a behavior corresponds to noninteger $n<1$ and $n<2$, respectively.

[6]R. Lipowsky and M. E. Fisher, Phys. Rev. Lett. **57,** 2411 (1986); Phys. Rev. B **36**, 2126 (1987).

[7]R. Lipowsky and S. Leibler, Phys. Rev. Lett. **56,** 2541 (1986); **59,** 1983(E) (1987); in Ref. 1, p. 98.

[8]If the two surfaces are characterized by the elastic parameters K_1 and K_2, one has $K=K_1K_2/(K_1+K_2)$ in Eq. (1).

[9]The rescaling of R and $\bar{R}$ involves T: $\rho\sim RT^{-1-\tau/2}$ and $\bar{\rho}\sim\bar{R}T^{(\tau-3)/2}$

[10]R. Lipowsky, Europhys. Lett. **7,** 255 (1988); in Ref. 3.

[11]K. G. Wilson, Phys. Rev. **B 4**, 3184 (1971); K. G. Wilson and M. E. Fisher, Phys. Rev. Lett. **28,** 240 (1972).

[12]F. Wegner, in *Phase Transitions and Critical Phenomena,* edited by C. Domb and M. S. Green (Academic, London, 1976), Vol. 6.

[13]A parabolic flow is also contained *within the critical manifold* of the q-state Potts model with a dilution field, say ψ, where q and ψ correspond to ρ and $\bar{\rho}-\bar{\rho}_{ES}$, respectively. This can be inferred from B. Nienhuis, A. N. Berker, E. K. Riedel, and M. Schick, Phys. Rev. Lett. **43,** 737 (1979); M. Nauenberg and D. J. Scalapino, Phys. Rev. Lett. **44,** 837 (1980).

[14]For a review, see M. E. Fisher, in *Critical Phenomena,* edited by F. J. W. Hahne, Lecture Notes in Physics Vol. 186 (Springer-Verlag, Berlin, 1983).

[15]Strictly speaking, the interactions $V(l)$ considered here which satisfy $V(l)=\infty$ for $l<0$ should not grow faster than a power law for small $l>0$. However, this should be an artifact of the RG procedure used here.

[16]R. Lipowsky and T. M. Nieuwenhuizen, J. Phys. **A 21**, L89 (1988).

[17]This follows from the singular part of the surface free energy, $f_s\sim 1/\xi_\parallel^{\zeta\tau}\sim(\bar{\rho}_c-\bar{\rho})^{\nu_\parallel\zeta\tau}$, with $\nu_\parallel\zeta\tau\geq 1$

[18]M. E. Fisher and M. Gelfand (to be published) discuss this subregime in terms of random walks.